

The effect of PMF Camel Urine Nanoparticles on A549 Cells: The Mechanism of Action and Drug DeliveryGehan A-R. Ahmed^{1,2,3*}, Faten A. Khorshid^{4,5}, Alaa Khedr⁶, Salem M. El-Hamidy⁵, Numan A. Salah⁷¹Biochemistry Department, Science College, King Abdulaziz University, KAU, Jeddah –KSA²Medical Biophysics Research Lab. -King Fahd Medical Research Centre, KAU, Jeddah –KSA³Spectroscopy Department, Physics Division, National Research Centre- Cairo, Egypt⁴Tissue Culture Research Unit, King Fahd Medical Research Centre, KAU, Jeddah –KSA⁵Biology Department, Science College, KAU, Jeddah –KSA⁶Faculty of Pharmacy KAU- Pharm. Dep Assuit University-Egypt⁷Center of Nanotechnology, King Abdulaziz University, Jeddah-KSAjahmed@kau.edu.sa, gehan_raouf@hotmail.com

Abstract: PMF is a natural selective anticancer, fraction extracted from camel urine (PM701), resemble in their actions the new drugs now used and manufactured in nanomedicine and nanotechnology. The PMF nanoparticles and its effect on the lung cancer cells A549 were studied by scanning electron microscope (SEM), Transmission electron microscope (TEM), energy dispersive X-ray (EDX) and the vibrational spectroscopy. A549 were treated with PMF for 2, 5, 10, 20 seconds and 1 minute. Fourier transforms Infrared Spectroscopy (FTIR) and TEM were used to study the membrane lipid profile and the morphology of the treated cells. The results revealed that several ions that present in a relatively high concentration in PMF were confirmed such as K, Ca, Cd, Y, Eu, Th and zinc, zinc is present in form of ZnO and Ca, Cd & Y are in form of sulfates as confirmed by the oxide and sulfate bands in the FTIR spectrum of PMF. Arginine, hippuric and benzoic acids as well were also detected. The PMF contains different types of macro and nanoshells with different types of metals that attack first, the A549 cell membrane and influenced the membrane polarity, packing and the hydrocarbon chain length of the phospholipids. These changes were indicated by the changes in the asymmetric stretching CH_2/CH_3 , symmetric stretching of membrane CH_2/CH_3 , symmetric stretching CH_2 /total lipids ratios respectively. Second, these nanoparticles directed after endocytosis to the nucleus and other cell organelles some of these metals are responsible for the selectivity of PMF fraction to cancer cells only. This new smart drug based on the most new frontiers in nanotechnology which include nanoshells as drug carrier.

[Gehan A-R. Ahmed, Faten A. Khorshid, Alaa Khedr, Salem M. El-Hamidy, Numan A. Salah. **The effect of PMF Camel Urine Nanoparticles on A549 Cells: The Mechanism of Action and Drug Delivery.** *Life Sci J* 2015;12(7):63-75]. (ISSN:1097-8135). <http://www.lifesciencesite.com>. 8

Keywords: A549 Lung cancer cells, Nanomedicine, PMF, Vibrational Spectroscopy, Membrane lipids, Electron Microscope, LCMS /GCMS, LC-MSMS – IonTrap, Cancer treatment.

1. Introduction

The most common use of nanotechnology on medicine has been in areas of developing novel therapeutic and imaging modalities¹. Intelligent drugs are the new agents that could potentially allow increased cancer selectivity, changes in pharmacokinetics, amplification of cytotoxic effects.^{2,3} The drug used in chemotherapy has a narrow therapeutic index. In contrast, targeted therapy that directed specifically against cancer cells and signaling pathways proved to limit nonspecific and toxicities. Thus, targeted therapies represent a new and promising approach to cancer therapy, one that is already leading to beneficial clinical effects.⁴

As the physical scale of nanomaterial is of the same order as viruses one might expect they will have highly variable interactions with cells and tissues dependent on their size, shape, surface patterning, and charge.⁵ An important goal in nanomedicine is to combine several of the special features of materials to improve the selectivity and the agent's therapeutic

index. The simplest way to achieve this is by combining the functions of targeting and killing with cytotoxic missile.⁶ Camel urine is rich in many organic and inorganic compounds. PMF is a fraction extracted from PM701 camel urine that proved to be highly selective agent for many types of cancer in tissue culture levels and in the animal model as well.⁷⁻⁹ It has been tested on healthy volunteers and passed the clinical trial phase I successively.¹⁰

In this study we tried to explore various PMF Nanoparticles structure and their mechanism of action on A549 cells when treated with PMF at different time intervals ranging from 2sec up to 1 min by using SEM, TEM, Raman microscopy, FTIR, SEM-EDX, LCMS /GCMS and LC-MSMS – IonTrap

2. Materials and Methods

The experimental work of the present study was conducted at the Medical Biophysics Laboratory at King Fahd Medical Research Center, King Abdulaziz University, Jeddah, Kingdom of Saudi Arabia.

A. Scanning Electron Microscopy (SEM)

For SEM studies the PMF was suspended in distilled water, then treated in an ultrasonic bath (BRANSON, 1510) about 20 min. A small drop of this suspension placed on the double side carbon tape on Al-Stub and dried in air. The specimens were analyzed - without gold coating- by using energy dispersive analyzer unit (EX-23000BU) which attached to the scanning electron microscope (JSM-6360LA, JEOL, Tokyo, Japan). The microscope was operated at an accelerating voltage of 20 kV. Quantitative method ZAF, and characterization method as pure.

B. LCMS/GCMS, LC-MSMS – IonTrap

High-performance liquid chromatography-with Ion Trap 6320 MSMS (LC-MS) from Agilent (HPLC-1200 series quaternary pum, solvent selector, degasser, autosampler, column compartment, Ion Trap 6320 Agilent technologies, USA), the system and data integration were handled with Chemstation for LC-MS.

HPLC column was Agilent Zorbax Extend C18, 150 mm (length) x 4.6 mm (internal diameter), 5 µm (particle size), 80 Å (porosity). Pre-column used was, Agilent Zorbax Eclipsed XDB C18, 4.6 mm x 12.5 mm, 80 Å, 5 µm (Agilent Technologies, Palo Alto, CA, USA). The column oven adjusted at 35 °C.

The ion-Trap was set as follow: The MS-Ion trap system was calibrated from 15 to 2200 using Agilent tuning mix applying, in sequence, scan calibration, fragmentation calibration, and isolation calibration and defining positive ion-masses; 118.09, 322.05, 622.05, 922.01, 1521.97, 2121.93.

A gas chromatograph (GC)-mass spectrometer (MS), Clarus 500 GC/MS (PerkinElmer, Shelton, CT) was used. The software controller/integrator was TurboMass, version 4.5.0.007 (PerkinElmer). An Elite-5MS GC capillary column (30 x 0.25-mm x 0.5 µm, PerkinElmer) was used. Calibrant used was heptacos (15-650 m/z).

Screw capped autosampler vials (V-shaped 300-µL and 1.8 mL) were from Alltech (Alltech, GmbH, Unterhaching, Germany). Heating oven (Heraeus, Kendro, Hanau, Germany) was adjusted at 60 °C. Calibrated digital micro-transfer pipettes 5–250 µL, Brand, Wertheim, Germany, were used. Labufuge 200 Centrifuge 5300 rpm (Heraeus Kindro, Germany).

Chromatographic conditions**[A] A gas chromatograph (GC)-mass spectrometer (MS):**

The carrier gas was helium (purity 99.9999%) at a flow rate of 1.0 mL/min (32 p.s.i., flow initial 45.0 cm/s, split; 1:50). Temperature conditions were: inlet line temperature, 180 °C; source temperature, 170 °C; trap emission, 100 °C; and electron energy, 70 eV. The column temperature program was: 50 °C for 2 min, increased to 280 °C (rate, 20 °C/min), and held for 5 min. The injector temperature was 260 °C, MS scan was

performed from 50 to 400 m/z. The NIST Mass Spectral Program for the NIST/EPA/NIH Mass Spectral Library, version 2.0f, build Oct 8, 2008 USA was used for confirmation and identification of peaks. Matching probability of >50% were considered.

[B] LC-MS; For LCMSMS-Autoscan-TIC with Autofragmentation and smart fragmentation:

Mobile system-I (for separation and identification of major compounds): ammonium acetate, 0.05M (A), acetonitrile (B); pumped at flow rate of 0.2 mL/min as follow:

	Time, min	%A	%B
1	0 - 5	100	0
2	5- 60	0	100
3	61	100	0

Mobile system-II (for separation and identification of Estrogens):

Prepared by mixing 900 mL methanol, 99.5 mL water, and 0.5 mL formic acid, filtered through 0.45 µm Nylon membrane, degassed and pumped at a flow rate of 0.2 mL/min. Injection volume is 20 µL

[C] Ion-trap mass conditions for LC-MSMS-MRM;

The MS parameters were defined as follow; peak width 2.0, isolation = on, fragmentation = off, Nebulizer 25 psi, Dry gas 11 L/min, Temperature 350 °C, m/z range and target mass was selected based on the MSMS operation, max accumulation time 200 MS ramp range 4500 – 1500 v. The MS Chromatogram was then retrieved and integrated using AUTO- MS mode for Total-Ion Chromatogram of the selected m/z (All-TIC-MS-n). Peaks were verified by m/z and retention time. Major ion MS peaks were selected as candidate for direct MSMS and fragmentation at different voltages. The MSMS data of each single ion was then matched with NIST2008. The Identified peaks were then analyzed by LC-MS applying MRM mode (Mixture Reaction Monitoring).

For direct MSMS the Ion-Trap conditions adjusted to; Nebulizer 15, Dry Gas 7, Temp 325 °C, fragmentation voltage 0.2 – 8.0 V (default 1.0V).

Procedure:

[A] About 50 mg of PMF was dissolved in 2 mL water.

[A-1] This sample was checked for the major constituent without any modification. Part of this sample (1 mL) was transferred to syringe-pump for direct MSMS. Direct MSMS analysis was performed to estimate the major ions that NOT observed in blank injection (water). A list of major ions was written and checked by MSMS-Single ion monitoring with fragmentation / isolation applying variable voltages (0.1 to 8V). Each single trapped ion was left 5 minutes to run for fragmentation with a flow rate of 5 µL/hour.

The saved files were downloaded and the $\sum MS(n)$ was retrieved and investigated for similarity and matching with NIS-MSMS-Ion-Trap library (applying the same fragmentation voltage as per the library).

[A-2] A gradient LC elution program was applied with Auto-MSMS mode for the detected peaks over the threshold of average noise level of TIC-Baseline. By this procedure we could also confirm the major constituents with characteristic MSMS, which is then checked for similarity with the NIST-MSMS-Ion Trap data. Elution was programmed to deliver 100% 0.05M ammonium acetate pH 6.5 for 5 min, then to 100% acetonitrile within 55 min, at a flow rate of 0.2 mL/min.

[B] Enzymatic hydrolysis, sample preparation and analysis:

This procedure was applied to investigate the conjugated compounds. This enzyme is used to hydrolyze any glucuronides or sulphate conjugated compounds.

In a glass test tube (15-mL with screw cap) A weight of 500 mg of PMF was dissolved in 1 mL water and 2 mL 0.1M sodium acetate (pH 5.5), and mixed with 100 μ L β -glucuronidase arylsulphatase. The reaction mixture was left for 24 hours at 42 °C in water bath thermostatically controlled. The mixture was cooled and extracted with 10 mL dichloromethane. The organic layer was separated and evaporated by bubbling nitrogen gas over a water bath at 50 °C. The dried extract was reconstituted in 400 μ L dichloromethane, and divided to two portions. One microliter from the first portion was injected for GC-MS analysis and then the remaining amount was derivatized with MSTFA and analyzed by GC-MS. The second portion was dried again under N₂ gas and reconstituted with 200 μ L acetonitrile. This solution was subjected to direct LC-MSMS analysis (Auto MSMS/Scan/Fragmentation), LC-MSMS-Autofragmentation (for identification, using mobile system-I), and analysed for searching estrogens (dansylation procedure, using mobile-II).

The confirmed compounds were then analyzed by LC-MSMS using MRM mode, maximum 10 ions, to confirm the chromatographic profile of each compound, with a maximum of 3 overlapped peaks. MRM was applied for the analysis of different PMF batches to identify the average/ limit and the incidence of impurities.

B. Tissue culture

[A]. Media

The following commercially available media were prepared according to published literature, these include: Ordinary media, Minimal essential medium (MEM) (10%FCS): MEM is a rich, multipurpose medium that was used for cultivation of human lung cancer cells (A549). Phosphate Buffer Saline (PBS) is a Phosphate-Buffered physiological Saline solution.

Calcium and Magnesium free Solution Trypsin¹¹. Examined media: PMF (extracted from PM 701) is a natural product, easily available, cheap, sterile, and non-toxic according to our chemical and microbiological testing. PMF added to the ordinary media with ratio 2.5 μ g : 1 ml media

[B]. Human Lung Cancer Cells line:

Human Lung Cancer Cells, non- small cell carcinoma (A549) was obtained from cell strain from (ATCC) American Type Cultural Collection, available in the cell bank of Tissue Culture Unit, King Fahd Medical Research Center (KAU, Jeddah).

In vitro proliferation of cells

1. Human Lung Cancer Cells (A549) were suspended in culture medium MEM.

2. The cells were dispensed in 3X (6wells plate), 1x10⁵/ml in each well.

3. Each group of cells was incubated 24 hrs in suitable media and apoptosis was induced by incubating cells in PMF at different time points [2, 5, 10, 20seconds and 1 minute].

D. Transmission Electron Microscope

Fixation of A549 cells

1-Fix in Trump's fixative for ½ to 1 hr which is prepared as follows:

40 ml of the 50% glutaraldehyde, 800 cc of 0.2 M Sodium cacodylate buffer, 30 ml of 37% Formaldehyde Mix well and adjust the pH to 7.2 then add buffer to make a final volume of 1000 cc. Aliquot 10 cc into red top tubes, label as Trump's Fixative/ poison and store the tubes in rack in refrigerator.

2-Rinse cells twice in distilled water for 15 min

3-The Agar- Enrobement procedure as described elsewhere¹² and summarized as follows: Lightly we centrifuge the culture/fixative mix at room temperature to generate a very loose pellet after Trump's fixation. We removed carefully the supernatant and gently flow several milliliters of buffered glutaraldehyde /formaldehyde fixative, at room temperature onto the loose pellet of cells. After 15 min, lightly we centrifuge the cells to form a loose pellet and remove the fixative using a pipe with taking care not to aspirate the cells. Using a warmed plastic pipet, quickly transfer approx.. 50 μ L of warm agar onto the loose cells and gently stir the cells with the tip of the plastic pipet to suspend the cells in the warm agar. The tubes containing the suspended cells were placed in refrigerator until the agar solidifies. We put several milliliters of buffer into the tubes and used a spatula to dislodge the agar plug containing the cells. The agar pieces containing the enrobed cells were transferred into Petri dish containing buffer and trim the agar into 1 to 2 mm cubes.

4-Cells were post-fixed in Osmium tetroxide for ½ to 1hr. Rinse cells twice in distilled water 15 min each. Uranyl acetate for 20 min.

5-Dehydration: the cells were dehydrated through graded ethanol series (70%, 95% for 15 min, three times with 100% ethanol for 10 min and two changes of Propylene oxide for 8 min each.

6-Propylene oxide: resin (equal volumes 1:1) 30-45 min. Resin infiltration pure 30-45 min.

7-Embedded in pure resin into blocks at 60C overnight

E. Infrared spectroscopy

At various time points, the cells treated with PMF were harvested and washed twice (by centrifugation for 3 min at 300 g). The cell pellet was kept at -80 C and lyophilized prior to IR measurements. The lyophilized samples – from three different separated experiments - were dispersed in potassium bromide (KBr) discs by mixing them gently in an agate mortar and with pestle to obtain homogenous mixture as described earlier.^{13, 14} The mixture then pressed in a die at 5 metric tons force for 10 s, creating a 1.1 cm diameter transparent disc with imbedded sample. The FTIR spectra were recorded in absorbance form using Shimadzu FTIR-8400s spectrophotometer with continuous nitrogen purge. The spectra were obtained in the wavenumber range of 4000-400 cm^{-1} with an average of 20 scans to increase the signal to noise ratio and at spectral resolution of 4 cm^{-1} . All the samples were baseline corrected and normalized to amide I band by using IR Solution software. Infrared spectrum of PMF sample was also obtained in potassium bromide (KBr) discs.

F. Raman Microscopy

Raman spectrum was measured using a DXR Raman Microscope, Thermo Scientific, using a 532 nm laser as the excitation source at 600 mW power. The PMF sample was dissolved in distilled water. The spectrum was accumulated over 5 min with 300 scans.

G. Chemicals

PMF fraction was prepared by from Camel's urine as dried brownish past. Dansyl chloride (Dns-Cl, $\geq 99.0\%$ HPLC for fluorescence BioChemika) was purchased from Sigma-Aldrich, (Sigma-Aldrich, St. Louis, MO, USA). β -glucuronidase/arylsulfatase (Helix pomatia, Type HP-2 ≥ 500 Sigma units β -glucuronidase and ≤ 37.5 units sulfatase activity) was obtained from Sigma Chemical Co. (St. Louis, MO) All solvents used were of HPLC grade. Sodium acetate trihydrate and formic acid were of Analytical grade. N-Trimethylsilyl-N-methyl trifluoroacetamide, MSTFA, $>98.5\%$ GC, was purchased from Sigma-Aldrich, Germany. Reference standard of Estrogens and 5 potential metabolites were purchased from STERALOIDS; Estrone (E1), Estradiol (E2), and Estriol (E3), 2-MeOE1 (E4), 4-OHE1 (E5), 4-MeOE2 (E6), 16 α -OHE1 (E7) and 4-OHE2 (E8). All other chemicals and solvents were of HPLC grade (BDH, London, England).

3. Results and discussion

Camel urine is rich in many organic and inorganic compounds. We will focus here on some parts not all of the PMF structure that may explain its role and selectivity in inducing apoptosis to A549 cells.

PMF Surface Morphology

To examine the surface morphology of PMF we used the Scanning Electron Microscope (SEM). PMF images (Fig. 1) demonstrated different nanoparticles, crystals, and nano-rods with varying shapes and sizes. Nanoshell particles with different diameter were found to be in the size range of ~26, 34, 41, 57nm and up to 150 nm were also seen. PMF SEM images of the crystals indicate the presence of Calcium oxalate, Cystine, Tyrosine, Uric acid crystals in addition to Ammonium urate and Calcium Phosphate. El-Shahawy¹⁵ detected earlier the presence of Glycine, Alanine, Arginine in PMF. Receptor tyrosine-specific protein kinases are a subclass of cell-surface growth-factor receptors with an intrinsic, ligand-controlled tyrosine-kinase activity. They regulate varied functions in normal cells and have a vital role in oncogenesis.¹⁶ Tyrosine kinases are an especially important target because they play an important role in the modulation of growth factor signaling.⁴ Glycine and cyctine are amino acids that enter to glutathione structure. Glutathione is the famous antioxidant in the body, depletion of this small tripeptide molecule will lead to the accumulation and increased reactive oxygen species and consequently affect the immune system.¹³ Thus, presence of tyrosine enhance the targeting and selectivity of PMF to cancer cells and the presence of Glycine and Cytine are amino acids improve the immune system to kill cancer cells. In addition, PMF has many cluster of rods attached in such strange pattern (Fig. 1H) may be due to a magnetic effect.

PMF major constituents

The PMF major constituents confirmed by LCMS/GCMS, LC-MSMS – IonTrap were given in (Table 1-3). In addition to the previously mentioned amino acids arginine was detected and hippuric and benzoic acids as well. The role of the L-arginine/nitric oxide (NO) pathway in tumor therapy has been well-studied. Members of this pathway have been reported to be promising and targeting therapeutic molecules in tumor therapy.¹⁸ Furthermore, arginine has several immunomodulatory effects such as stimulating T- and natural killer cell activity and influencing pro-inflammatory cytokine levels. This may be through activation of interleukin -12 (IL-12).¹⁹ Moreover, it has been reported that induction of IL-23 leads to the production of interferons (IFNs) and other tumor-suppressive factors. These molecules are

activated as part of the antitumor immunity response and promote apoptosis to tumor cells.²⁰

The International Immunology Foundation (IIF) is dedicated to the study of the relationships between the immune system of the patient and his or her cancer. Their goal is to enhance and unblock immune function so as to help this elegant system to successfully deal with cancer. The immune suppression that is generated by the cancer cell to protect itself from the patient's immune system can be removed. When the patient's immune system is unblocked it can identify and destroy cancer cells. A mature technology that removes immune suppression in cancer patients is Immunopheresis and it is important than stimulating the immune system (IIF). Three decades ago M. Rigdon Lentz, MD and others established this technique. They showed that cancer cells produce soluble inhibitors that block the tumor cytotoxicity of tumor necrosis factor (TNF). These inhibitors can be removed from the blood safely and efficiently; and that once removed, the unblocked immune system can rapidly kill cancer cells. In clinical experience to date

this immune unblocking has yielding significant clinical responses, including complete tumor remissions (IIF).

Tamás²¹ studied the effect of mixtures of amino acids and other small molecules in cancer patients. They found that administration of the product to cancer patients significantly improved their quality of life but they did not investigate the anticancer activity of these products. By contrast, Gyula²² detected inhibition ranging between 40% to 69% in mice tumor when treated with active mixture of amino acids that possesses a selective toxic effect on tumor cells in vitro and in vivo. Gyula²³ tested the potentiating effect of D(+)- mannose, orotic, and hippuric acid sodium salt on selective toxicity of circulatory system in culture for various tumor cell lines and found these compounds have play part of the defense system. Lei²⁴ proved the effect of cinnamic acid as a natural product that has anti-tumor activity. They revealed this activity in part to the inhibition of protein isoprenylation known to block mitogenic signal transduction.

PMF major elements

Table 1: Compounds in PMF confirmed by LC-MSMS – IonTrap

tR [min]	Compound Name	Area	Max. m/z(MH+)	Height	Area%
13.999	HIPPURic acid	2144039484	179.92	52552031	45.5
15.12	Phenacet URic acid	1311173081	193.92	41727416	27.8
5.082	CREATINine	1101779506	114.05	23867673	23.4
3.449	Phenyl-3-propyl	64659341	136.85	3168430	1.4
26.881	Alpha-biSABolol	43726530	222.89	3332237	58.2
7.732	Benzeneacetic acid	29811100	136.94	922491	0.6
20.657	PROSTAGLANDIN E2	28044617	353.16	3376173	37.3
18.399	CRYSol	26160372	109.10	531737	0.6
18.377	BenZoic acid	18109930	123.06	674079	0.4
36.641	Cis-5,8,11-Eicosatrienoic acid	3416775	306.98	230195	4.5

Table 2: PMF major constituents. Compounds confirmed by GC-MS (not TMS-derivatives), enzymatically hydrolyzed sample

tR, min	GC-MS Confirmed compound	M+
8.97	Phenol, 2-(ethylamino)-4-methyl-	151
7.8	Phenol, 2-pentyl	164
7.49	Benzoic acid, 2-amino-, methyl ester	151
6.93	Phenol, 3-propyl-	136
6.45	1,2-Benzenediol	110
6.24	Phenol, 3-ethyl-	122
4.6	Phenol	94
5.5	o-Cresol	108

To identify the possible elements that could be present in PMF we tested it with Energy Dispersive X-ray (EDX) (Fig. 2) and with Inductively Coupled Plasma/Mass Spectra (ICP/MS) (Table 4). We identified several ions that present in PMF in a relatively high concentration such as K, Ca, Cd, Y, Eu, Th and zinc, zinc is present in form of ZnO and Ca, Cd & Y are in form of sulfates as confirmed by the oxide and sulfate bands in the FTIR spectrum of PMF (Fig. 3). The FTIR

spectrum of PMF in the range of 4000-400cm⁻¹ which showed the characteristic bands of glycine indicated by the amide absorbance doublet bands in the range 1500-1700cm⁻¹. Zinc is present in the form of ZnO indicated by the IR absorbance band around 567cm⁻¹. Sulfate ions are observed at 1074, 1137cm⁻¹ while carbonate ions around 1030 and 830 cm⁻¹. We thought that PMF selectivity may be due to many factors such as the presence of ZnO nanoparticles, and/or Cs and Rb at

alkali pH.⁹ The novel findings of cell selective toxicity towards potential disease causing cells indicate a potential utility of ZnO nanoparticles in treatment of

cancer and/or autoimmunity.²⁵ Cd and Y may be the core of nanoshell Y has a high magnetic properties.

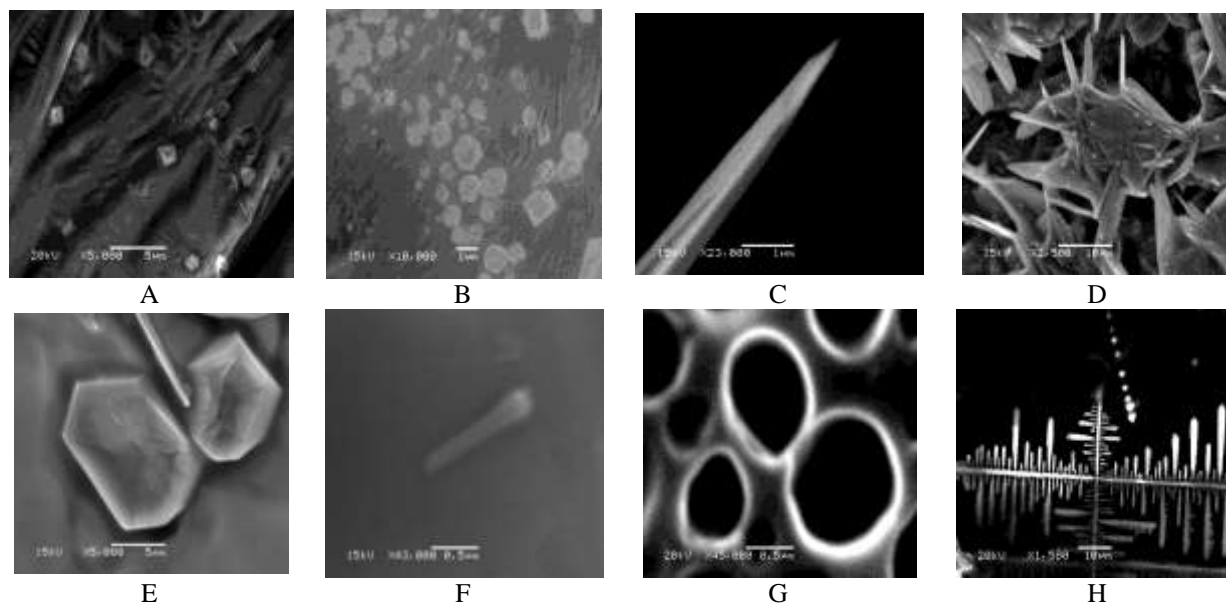


Fig.1. SEM images of PMF showed the presence of A) calcium oxalate crystals, B) Cystine crystals, C) Tyrosine, D) Uric acid crystals, E) Ammonium urate, F) Calcium Phosphate, PMF nanoshells with different diameters (G) and clusters of nano-rods connected and arranged in tremendous pattern due to magnetic effect (H).

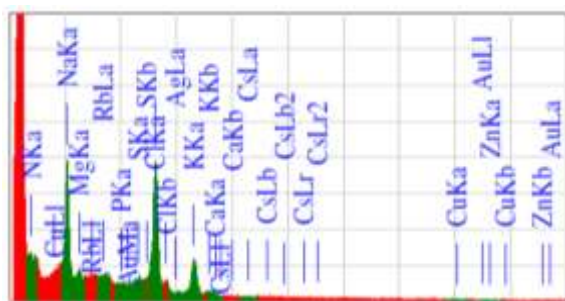


Fig. 2. The EDX patterns show the abundant elements found in the PMF examined by SEM-EDX.

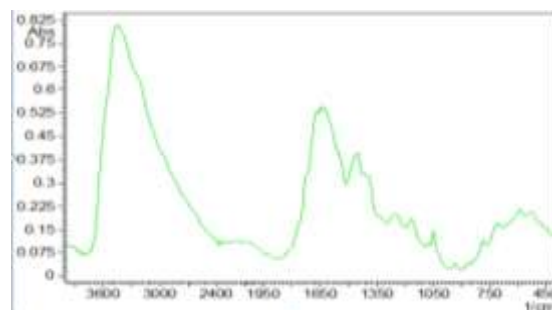


Fig. 3. The FTIR spectrum of PMF in the range of 4000-400 cm^{-1} which showed the characteristic bands of glycine indicated by the amide absorbance doublet bands in the range 1500-1700 cm^{-1} . Zinc is present in the form of ZnO indicated by the IR absorbance band around 567 cm^{-1} . Sulfate ions are observed at 1074, 1137 cm^{-1} while carbonate ions around 1030 and 830 cm^{-1} .

Table 3: PMF major constituents. Compounds confirmed by GC-MS as TMS derivative, enzymatically hydrolyzed sample

Glycine, N-(trimethylsilyl)-, trimethylsilyl ester	219	
Benzenepropanoic acid, trimethylsilyl ester	222	8.06
Benzenoacetic acid, trimethylsilyl ester	208	7.24
dl-3-Aminoisobutyric acid, trimethylsilyl ester	175	7.17
Benzoic acid trimethylsilyl ester	194	6.9
3-Ethylphenol, trimethylsilyl ether	194	6.87
Silane, trimethyl(3-methylphenoxy)-	180	6.17
Silane, trimethylphenoxy-	166	5.4

PMF internal morphology

In an attempt to explore the internal morphology of PMF we used Transmission Electron Microscope (TEM) (Fig. 4). Interestingly, we found several spherical nanoparticles in form of nanoshells with diameter range between 26 up to 57nm. Nanoshells and dendrimers nanodelivery systems are synthesized to allow more specific targeting of the drug in treating cancer to minimize its side effects.²⁶

Polyamidoamine (PAMAM) dendrimers contain tertiary amines and amide linkages which allow for binding of numerous targeting and guest molecules.²⁷

Examining of PMF in liquid form with Raman microscope (Fig. 5) revealed that PMF consists of different microshells with multilayers and different cores.

The Raman spectra obtained from different shells and the light core revealed that the outer and inner shells have the same spectrum. Moreover, almost the shell and the light core have the same structure (Fig. 6). The light core has little differences in the band intensity around 1030, 567 cm^{-1} indicating an increase in carbonate and ZnO concentrations in the light core compared to the shell. The Raman spectrum of the dense core gives information about the constituent of this core which indicates the presence of magnetic core of Ytterbium (III) sulfate.

V. The mechanism of PMF nanoparticles insertion into A549 cells

In order to evaluate the high efficiency, target specificity and to find out the mechanism of PMF in inducing apoptosis to A549 cells we took the FTIR spectra (Fig. 7) and TEM imaging (Fig. 8) to these cells after 2, 5, 10, 20 sec, and 1min of PMF treatment. FTIR spectroscopy is proved to be a valuable sensitive analytical technique. It gives qualitative as well as quantitative information of the chemical functional groups and the secondary structure of proteins¹⁴. The CH stretching vibration modes over the range 3000-2800 cm^{-1} comprises mainly the CH_3 and the CH_2 asymmetric and symmetric modes of vibrations of fatty acids and the acyl chain.

In order to investigate the membrane polarity, packing and the hydrocarbon chain length of A549 cells prolong the treating time, we calculated the intensity ratios $I(2921\text{cm}^{-1})/I(2871\text{cm}^{-1})$, $I(2852\text{cm}^{-1})/I(2871\text{cm}^{-1})$, and $I(2925\text{cm}^{-1})/\text{total lipid (asCH}_2\text{+sCH}_2\text{)}$ from the FTIR spectra of the treated cells with the positive control A547 cells (Table 5) respectively. The membrane polarity and packing decreased significantly in all treated cells for different times; the minimum values were detected for cells treated for 1min while cells treated for 5 sec showed a relatively higher values in these ratios compared to the other treated cells although they still have lower values compared to the control A547 cells. This increase in the

membrane fluidity may be due to the presence of, K^+ , Ca^{2+} , Eu^{3+} ions. Same results was obtained by Fan²⁸ when detected a decrease in the rigidity of acyl chains of phosphatidylcholine (PC) and bovine serum albumin (BSA) complex when used these ions as a membrane model to study the interaction of metal ions with membrane lipid.

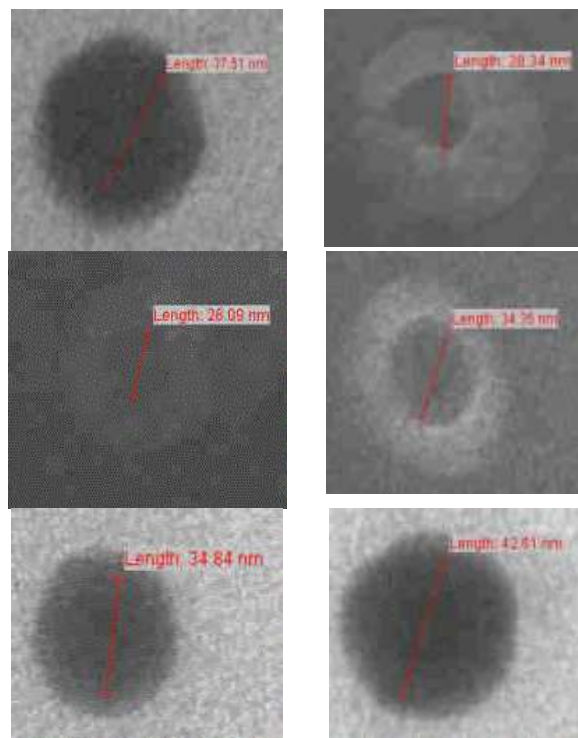


Fig. 4. TEM images demonstrate the internal structure of PMF nanoparticles. Spherical nanoshells with different diameters and different cores; light and dense cores.

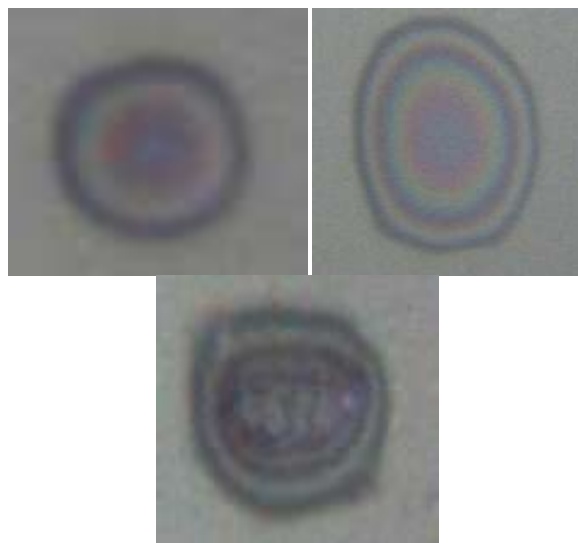


Fig. 5. FT-Raman microscope image of PMF fraction. The images show different microshells with multilayers and also light and dense cores.

Accompanied the increase in membrane fluidity we also detected an increase in the length of hydrocarbon chain as indicated by the increase in the $I(2925\text{cm}^{-1})/\text{total lipid ratio}$.

We next tried to determine whether the detected nanoparticles can invade and induce apoptosis to A 547 cells. Particle shape significantly impacts the cellular and tissue interactions of nanomaterials. Endocytosis of shapes that are non-spherical are highly dependent on the local shape at the interface of the cell with the nanomaterial or the tangential angle that nanomaterial shape makes with the cell.²⁹⁻³¹ PMF possesses, in addition to spherical nano particles, rods and spike like structures. Actually, the shape of the nanoparticles and the degrees of membrane fluidity during PMF treatment facilitate and play a great role in the nanoparticles endocytosis by the cancer cells.

Table 4. Part of the major PMF elements detected by ICP/MS.

Element	Mass	Concentration	SQ Unit	CPS
K	39	very high		over response
Na	23	7172.82	mg/l	28217881180
Mg	24	1137.07	mg/l	2154712288
Fe	56	4.95	mg/l	86920298.7
Sr	88	4.42	mg/l	53345799.21
Rb	85	1.77	mg/l	15917799.76
Zn	66	121.08	ug/l	460777.57
Mn	55	6.61	ug/l	78250.7
Pb	208	1.61	ug/l	96212.96
Co	59	1.09	ug/l	38824.97
Sb	121	687.29	ng/l	4320.78
Pd	105	600.20	ng/l	9232.95
Y	89	178.31	ng/l	4561.17
Hg	202	172.07	ng/l	1870.21
Cd	111	71.40	ng/l	390.03
Cs	133	48.78	ng/l	1200.1
Ag	107	38.07	ng/l	1720.17
Th	232	1.43	ng/l	90.01

The hypothesis that the army of PMF nanoparticles attacks A549 cells in successive stages or steps was made. First the cell membrane as early as 2sec post PMF treatment starts to be less packing with increasing the hydrocarbon chain length of its fatty acids and logically decreased the membrane polarity which in turn weekend the Wan der wall forces between the polar head groups and hence increases the membrane fluidity.

These findings have been proved by the FTIR calculated intensity ratios and morphologically by TEM images (Fig. 8). These enable the larger nanoparticles which possessed a relatively high content of negatively charged amino acids [aspartic & glutamic acids] to escape immediately inside the cell. The cells

engulfed specifically these nanoparticles and/or rods or spikes (Fig. 8A). After 5 sec the membrane restored part of its rigidity and polarity. Cancer cells are addicted to glycine; there are only a few clinically approved nanocarriers that incorporate molecules to selectively bind and target cancer cells³²; ; most probably glycine inter in the formation of the membrane of these observed nanocarrier. After the initial burst, a very fast nanoshells with different diameters released was observed together with different separate nanoshells that attack the nuclear membrane and the other cell organelles. Glycine is abundant in PMF as detected by GC/MS.

Thus nanoshells invade the cytoplasmic and nuclear membrane start to create transit pores after 5 sec of PMF treatment²⁹ (Fig. 8B). These temporary pores may allow the heavy nanocarrier particles and/or the carrier vehicle to escape easily through the cellular membrane and the nuclear envelope and hence drain its load inside the cells after 5, 10, and 20 sec (Fig. 8C). After 1 min all types of PMF forms was seen inside the cancer cells crystals, needles and nanoparticles (Fig. 8D). The nanoshells are completely paralyzing the cancer cells. Swollen and rupture or degenerated mitochondria are sign of apoptosis were seen in the figure.

We put another hypothesis that Y acquires its magnetic property when the negative ions and negatively charged amino acids traveling inside the cell between the negatively charged inner membrane and the positively charged outer nuclear membrane. By using Fleming's left hand rule thus, at any angel of insertion the Y based nanoparticle directed forward to the inside the cell i.e. undeviating to the nucleus. This explains the appearance of a cluster of these magnetic nanoparticles first, after 5 sec, the nuclear envelop was surrounded by huge number of nanoparticles and hence the process of pore formation starts.^{9,33}

Second, after 20 sec of PMF treatment, 7 connected aggregates appeared inside the cancer cells (Fig. 8 C) which were observed earlier in (Fig. 1H).

With regards to cancer treatment, most current anticancer regimes do not effectively differentiate between cancerous and normal cells.²⁵ This indiscriminate action frequently leads to systemic toxicity and debilitating adverse effects in normal body tissues including bone marrow suppression, neurotoxicity, and cardiomyopathy.^{34,35} QDs consists of a typical core/shell structure composed of heavy metals³⁶⁻³⁸ include a cadmium selenide or cadmium sulfide core coated with zinc sulfide shell.

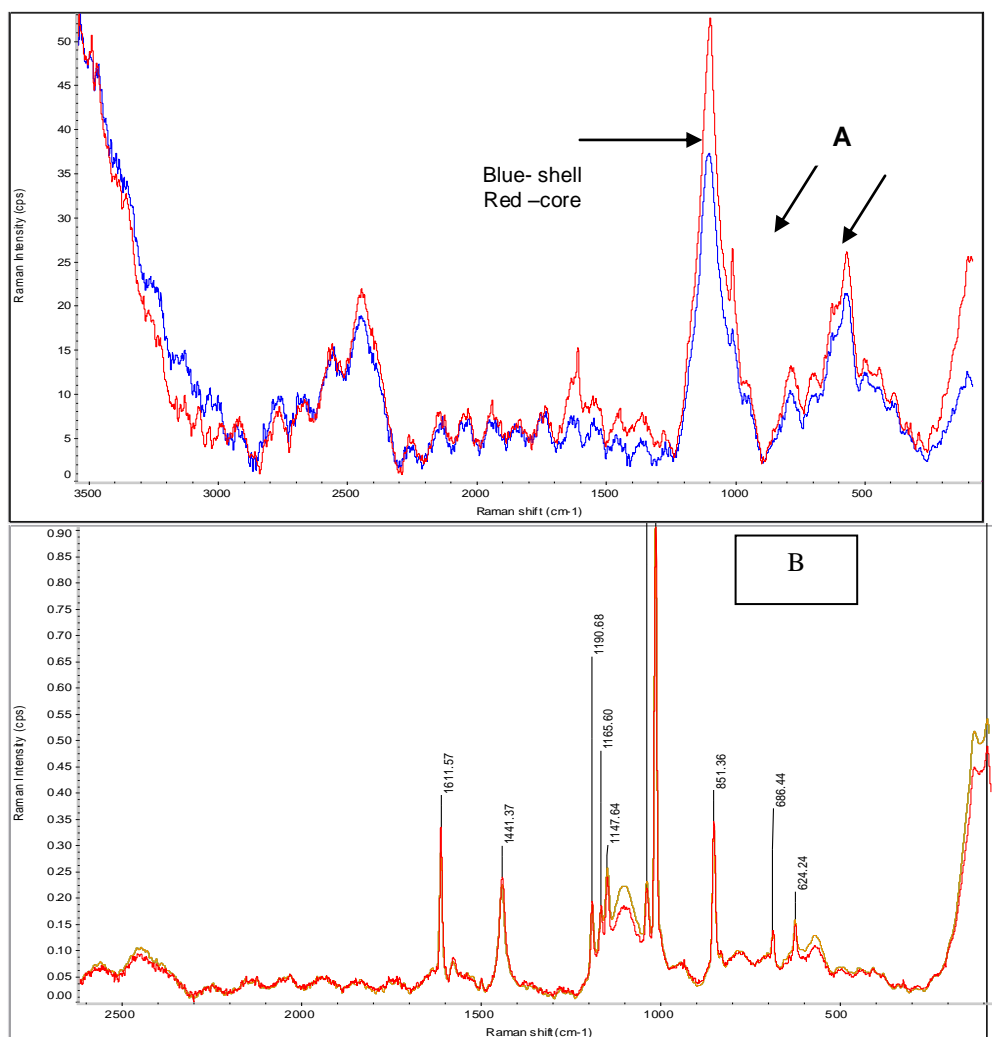


Fig 6. (A) The Raman spectra obtained from different shells and the light cores: The outer and inner shells have the same spectrum (left) while the shell and the **light** core have the structure but the core has a slight change in the band intensities of carbonate and ZnO bands (arrows-right). (B) FT-Raman spectra of different dense cores: The characteristic bands of CdSO₄ around 686,569 cm⁻¹, CaCO₃ Calcium carbonate around 1441, 850 cm⁻¹, thiocyanate bands at 2456, 2557 cm⁻¹, SiO₂ indicated by the presence of bands around 1100, 1147 cm⁻¹ and ZnO nanoparticle 567 cm⁻¹ were also detected in Raman spectrum of the dense core.

NPs applied as drug delivery systems are submicron-sized particles (3-200 nm), and are devices or systems that can be made using a variety of materials including polymers (polymeric NPs) micelles, or dendrimers), lipids (liposomes), viruses (viral NPs), carbon based nanostructures (nanotubes) and even inorganic/organic core/shell hybrid NPs³⁹. Various types of organic particles like liposomes and dendrimers should be mentioned, as these are already being used in cancer therapy and clinical treatment.⁴⁰ These synthetic nanoparticles match in their properties and action the PMF detected nanoparticles.

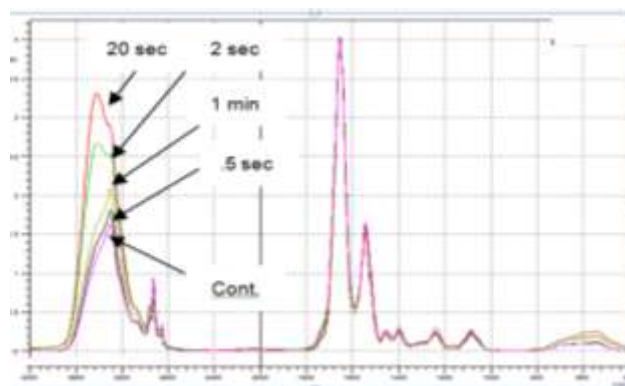
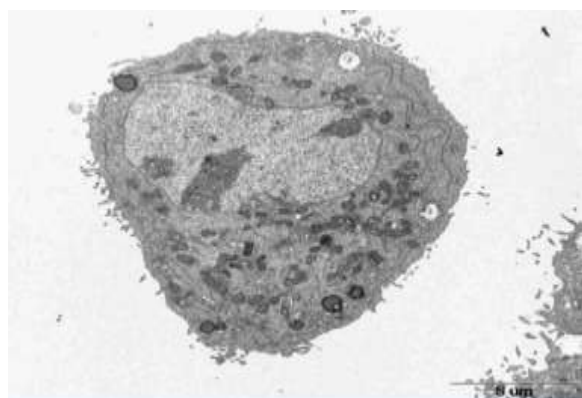


Fig. 7. The FTIR Spectra, in Kubelka Munk algorithm for clarity, of A549 cells at different time intervals of PMF treatment.

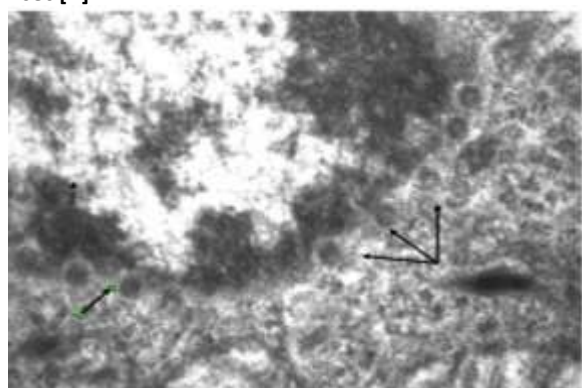
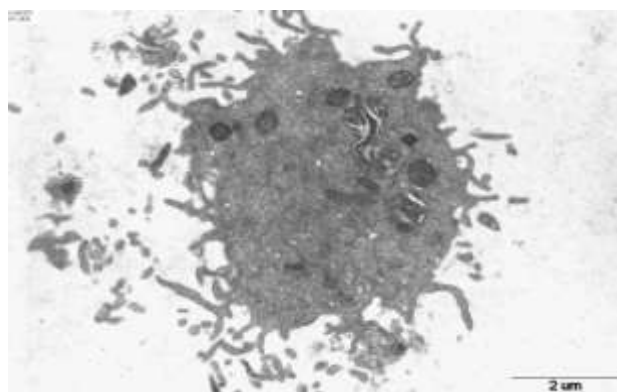
Table 5: The calculated intensity ratios obtained from FTIR spectra of the tested groups to indicate the membrane lipid polarity, packing and the hydrocarbon chain length.

Intensity ratio/ Tested time	cont	2sec	5sec	20sec	1min
as CH ₂ /sCH ₃ , I(2925cm ⁻¹)/I(2871cm ⁻¹) [lipid polarity]	1.787	1.676	1.753	1.690	1.676
s CH ₂ /sCH ₃ , I(2852cm ⁻¹)/ I(2871cm ⁻¹) Membrane packing	1.148	1.073	1.089	1.078	1.059
asCH ₂ /total lipids I(2925cm ⁻¹)/[total lipid] The hydrocarbon chain length	0.609	0.610	0.617	0.611	0.613

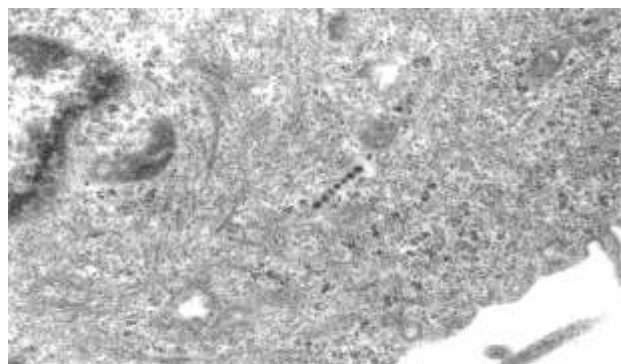
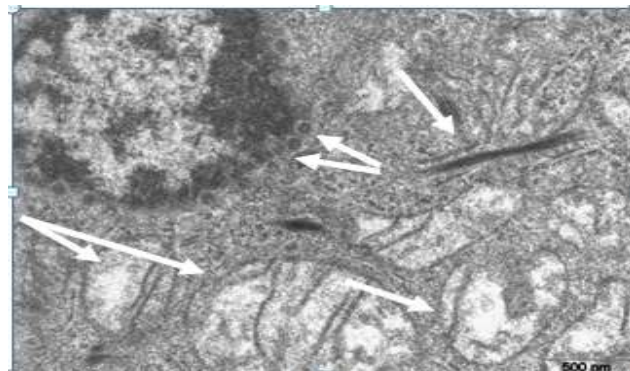
as= asymmetric, s = symmetric. The intensity values were taken from the average of three different measured IR spectra of each sample for each tested time.



2 sec [A]

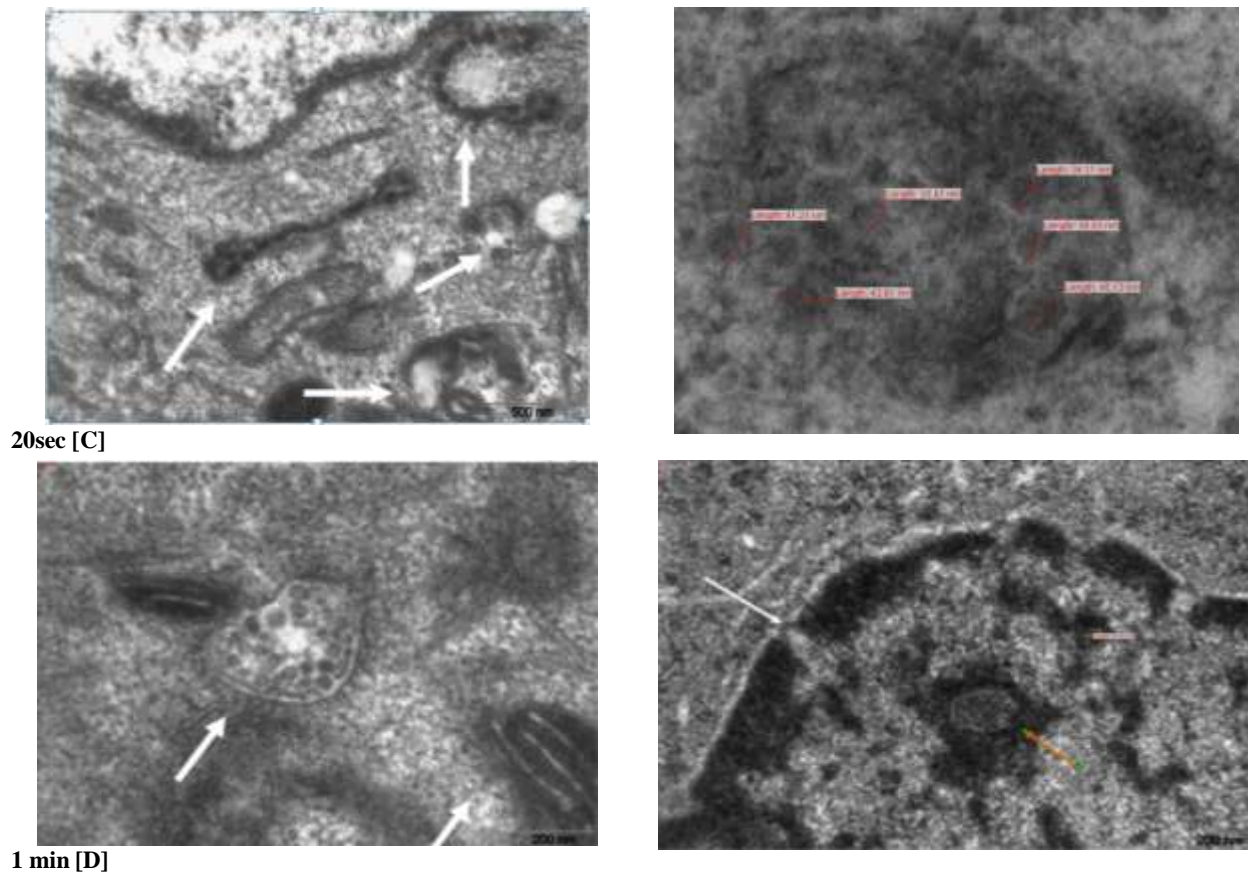


5 sec [B]



20 sec





1 min [D]

Fig. 8. A549 lung cancer cells after PMF treatment A) after 2 sec; spherical nanoparticles engulfed by the cells B) after 5 sec of treatment; Swollen and ruptured/degenerated mitochondria (sign of apoptosis), a spherical nanoparticles reach and invade the nuclear envelop and a nano rods was seen inside the cells. C) after 20 sec; larger nanocarrier and cluster of magnetic particles connected together inside the cells (left) and group of nanoparticles invade the lysosome of A549 cell or a cluster of nanoparticle inside a vesicle (right). D) after 1 min; (left) Nucleus completely occupied by nano particles, other cell organelles lose its features and structures, eg smooth endoplasmic reticulum (SER) have a diluted cistranae. Right) the nano particles of PMF surrounded the lysosomes, invaded the endoplasmic reticulum (ER) ER and damaged the Golgi apparatus (GA) and mitochondria. The figure also showed the presence of nanocarrier vessel loaded with nanoparticles inside the cancer cell after 20 sec and 1min of PMF treatment (yellow arrow).

5. Conclusion

PMF nanoparticles usually form a core of nanomaterial. They have surfaces for molecular assembly, that composed of inorganic materials revealed by the EDX, FTIR and FT-Raman spectra mainly Zn, Ag, Y, Cs, Rb. They are also in the form of nano-vesicle surrounded by a membrane layer or layers. The shape is often spherical with different sizes. The size and size distribution play an important role in certain situations. PMF possesses a variety of amino acids that makes with the above mentioned elements its unique selectivity to cancer cells. Thus, natural occurring nanoparticles obtained from PMF that have been passed phase I clinical trial, combines pH-triggered, drug-release and many of modes of selectivity offer a more targeted approach and

promises significant improvements in the treatment of cancer. These nanoparticles proved to induce apoptosis in A549 lung cancer cells.

Acknowledgments

The authors thank Nourah Alotaibi M.Sc. student, Tahani Dakhakhni (M. Sc.) in KFMRC – KAU for assistance with Raman and FTIR measurements; Hanady kashkary (M.Sc.) tissue culture unit- KFMRC – KAU for assistance with tissue culture. The authors thank also Mr. Helmy A. Shahab senior technician (research assistant) Electron microscope unit –KFMRC for assistance with TEM imaging. This work was funded by ALZAMEL Scientific Chair for Cancer Researches number "429/3/KBM.

References:

1. Frank, A., June-Wha, R., Jerome, P., Aleksandar, F., Radovic, M., Robert, L., Omid, C. New frontiers in nanotechnology foe cancer treatment *Urologic Oncology. Seminars and Original Investigations.* 26, 74-85 (2008).
2. Haberzettl, C. A. Nanomedicine: destination or journey? *Nanotechnology.* 13, R9 (2002).
3. Whitesides, G.M. The once and future nanomachine. *Sci. Am.* 285, 78-83 (2001)..
4. Amit, A., and Eric. M. Scholar, Role of Tyrosine Kinase Inhibitors in Cancer Therapy. *J. Pharma. Experm. Therap.* 315(3), 971-979 (2005).
5. Whitesides, G. M. The 'right' size in nanobiotechnology. *Nat. Biotechnol.* 2003; 21:1161-1165.
6. David, A. S., Carlos, H. V., Freddy, E. E., and Michael R. McD. Conscripts of the infinite armada: systemic cancer therapy using nanomaterials. *Nature Reviews Clinical Oncology.* 7, 266-276 (2010).
7. Khorshid, F.A. Preclinical evaluation of PM 701 in Experimental animals. *Int. J. Pharma.* 4(6), 443-451(2008).
8. Khorshid, F.A. Potential Anticancer Natural Product against Human Lung Cancer Cells. *Trends in Medical Research.* 4 (1): 9-15 (2009).
9. Faten, A. K., Gehan, A. R., Salem, M. El., Gehan, S. Al., Nourah A. Al., Taha A. K. PMF, Cesium & Rubidium Nanoparticles Induce Apoptosis in A549 Cells. *Life Sci. J.* 8(3):534-542 (2011).
10. Khorshid, F.A., Shazly, H., Al-Jefery A., and Osman, A.A. Dose Escalation Phase I Study in Healthy Volunteers to Evaluate the Safety of a natural product PM 701. *Int. J. of pharma. toxic.* 5(3): 91-9 (2010).
11. Giaever, I., Keese, C.R., *IEEE Transactions on Biomedical Engineering BME-33* (2), pp. 242-247, 1986.
12. *Methods in Molecular Biology-Electron Microscopy – Methods and Protocols*, 2nd Edition John Kuo, Humana Press- Totowa, New Jersey.
13. Paul, G. L., Robert, D. S., Cancer grading by Fourier transform infrared spectroscopy. 4, 37-46 (1998).
14. Raouf, G. A., Khorshid, F.A., Kumosani, T., FT-IR Spectroscopy as a Tool for Identification of Apoptosis-Induced Structural Changes in A549 Cells Dry Samples Treated with PM 701. *Int.J. Nano and Biomaterials.* 2(1/2/3/4/5), 396-408 (2009).
15. El-Shahawy, A., El-Sawi, N., Backer, W.S., Khorshid, F.A., and Geweely, N.S. Spectral Analysis, Molecular Orbital Calculations And Antimicrobial Activity Of PMF-G Fraction Extracted From PM-701. *Int. J. of Pharma and Bioscience.* 1(2):1-19 (2010).
16. Andreas, G., Oliver, M. F., & Axel, U., The discovery of receptor tyrosine kinases: targets for cancer therapy *Nature Reviews Cancer.* 4:361-370 (2004).
17. Gustavo, B. Whey protein concentrate (WPC) and glutathione modulation in cancer treatment. *Anticancer Research* 20, 4785-4792 (2000).
18. [Ma, Q.](#), [Wang, Z.](#), [Zhang, M.](#), [Hu, H.](#), [Li, J.](#), [Zhang, D.](#), [Guo, K.](#), [Sha, H.](#) Targeting the L-arginine-nitric oxide pathway for cancer treatment. [Curr. Pharm. Des.](#) 16(4):392-410 (2010).
19. Lin, W.W., Karin, M., A cytokine-mediated link between innate immunity, inflammation, and cancer. *J. Clin. Investig.* 117(5):1175-1183 (2007).
20. [Maria, M.](#), [Leslee, S.](#), [Harika, N.](#), [Michelle, P.](#), and [Fabian B.](#) Toll-Like Receptors as Novel Therapeutic Targets for Ovarian Cancer. *ISRN Oncology.* 2012 ID 642141, 8 pages(2012).
21. Tamás, C., Zoltán, L., Mária, B., Csilla, Z., Mária, G., Gyula K., Safety, Tolerability, and Effect on Quality of Life of a Mixture of Amino Acids and Other Small Molecules in Cancer Patients. *Cancer Biotherapy & Radiopharmaceuticals.* 29(3): 124-134 (2014).
22. Gyula, K., Dezső, G., Péter, I. K., Ákos, S., Tamás, C., A mixture of amino acids and other small molecules present in the serum suppresses the growth of murine and human tumors in vivo. *International Journal of Cancer.* 132(5): 1213-1221 (Mar 2013).
23. Gyula, K., PhD, Synergistic Potentiating Effect of D(+)- Mannose, Orotic, and Hippuric Acid Sodium Salt on Selective Toxicity of a Mixture of 13 Substances of the Circulatory System in Culture for Various Tumor Cell Lines. *Cancer Detectoin and Prevention.* 24(5), 485495 (2000).
24. Lei, L., Robert, W. H., Sonsoles, S., Mu, Q. Y., and Dvorit, S., Cinnamic acid: A natural product with potential use in cancer intervention. *International Journal of Cancer* 62(3), 345-350 (1995).
25. Cory, H., Janet, L., Alex, P., Reddy, K.M., et al., Preferential killing of cancer cells and activated human T cells using ZnO nanoparticles. *Nanotech.* 19(29), 295103 (2008).
26. Dhruba, J. B., Marianne, K. [...], and Shaker, A. M. Nanoparticles and cancer therapy: A concise review with emphasis on dendrimers *Int. J. Nanomedicine.* 4, 1-7 (2009).
27. Tomalia, D. A., Reyna, L. A. and Svenson, S. Dendrimers as multi-purpose nanodevices for

- oncology drug delivery and diagnostic imaging. *Biochemical Society*. 61-67(2007).
28. Fan, W., Zhanlan, Y., Yong, Z., Shifu, W., Li, Z., Jinguang, Wu. Influence of metal ions on phosphotidyl choline-bovine serum albumin model membrane, an FTIR study. *J. Molec. Str.* 794,1-11 (2006).
 29. Chithrani, B.D., Ghazani, A.A & Chan, W. C. Detrmining the size and shape dependence of gold nanoparticle uptake into mammalian cells. *Nano. Lett.* 6, 662-668 (2006).
 30. Champion, J. & Mitragotri, S. Role of target geometry in phagocytosis. *Proc.Natli Acad. Sci. USA* 103, 4930-4934 (2006).
 31. Zhang, K., Fang, H., Chen, Z., Taylor, J., Wooly, K. Shape effects of nanoparticles conjugated with cell-penetrating peptides (HIV Tat PTD) on CHO cell uptake. *Bioconjug. Chem.* 2008; 19:1880-1887.
 32. Dan, P., Jeffrey, M. K., Seungpyo, H., Omid, C. F., Rimona, M., & Robert, L. Nanocarriers as an emerging platform for cancer therapy *Nature Nanotechnology* 2, 751 – 760 (2007).
 33. Raouf, G.A., Khorshid, F.A., Kumosani, T.A. FT-IR Spectroscopy as a Tool for Identification of Apoptosis-Induced Structural Changes in A549 Cells Treated with PM 701. *Int.J. Nano and Biomaterials.* 2(1/2/3/4/5), 396-408 (2009).
 34. Nie, S., Xing, Y., Kim, G., Simons, J. Nanotechnology applications in cancer. *Annu. Rev. Biomed. Eng.* 9, 257-88 (2007).
 35. Bosanquet, A., Bell, P. Ex vivo therapeutic index by drug sensitivity assay using fresh human normal and tumor cells. *J. Exp. Ther. Oncol.* 4, 145-54 (2004).
 36. Michalet, X., Pinaud, F.F., Bentolila, L.A., Tsay, J.M., Doose, S., Li, J.J., et al. Quantum dots for live cells, in vivo imaging and diagnostic. *Science.* 307, 538-44(2005).
 37. Smith, A.M., Duan, H., Mohs, A.M., Nie, S. Bioconjugated quantum dots for in Vivo molecular and cellular imaging. *Adv Drug Del Rev.* 60, 1226-40 (2008).
 38. Rhyner, M.N., Smith, A.M., Gao, X., Mao, H., Yang, L., Nile, S. Quantum dots and multifunctional nanoparticles: new contrast agents for tumor imaging. *Nanomedicine.* 1, 209-17 (2006).
 39. Cho, K., Wang, X., Nie, S., Chen, Z., Shin, D., Therapeutic nanoparticles for drug delivery in cancer. *Clin. Cancer Res.* 14, 1310-6 (2008).
 40. Miriam, C., Fabio, C., Diego, F. HER2 targeting as a two-sided strategy for breast cancer diagnosis and treatment: Outlook and recent implications in nanomedical approaches. *Pharmacological Res.* 62(2), 150-165 (2010).

7/21/2015